DOI: 10.1007/s11099-018-0788-6 PHOTOSYNTHETICA 56 (1): 200-209, 2018

PsbY is required for prevention of photodamage to photosystem II in a PsbM-lacking mutant of *Synechocystis* sp. PCC 6803

S. BISWAS and J.J. EATON-RYE+

Department of Biochemistry, University of Otago, P.O. Box 56, Dunedin 9054, New Zealand

Abstract

The PsbM (3.9 kDa) and PsbY (4.2 kDa) proteins are membrane-spanning, single-helix, subunits associated with the chlorophyll-binding CP47 pre-complex of photosystem II (PSII). Removal of PsbM resulted in accumulation of PSII pre-assembly complexes and impaired electron transfer between the primary (Q_A) and secondary (Q_B) plastoquinone electron acceptors of PSII indicating that the Q_B-binding site and bicarbonate binding to the non-heme iron were altered in this strain. Removal of PsbY alone had only a minor impact on PSII activity but deleting PsbY in the ΔPsbM background led to additional modification of the acceptor side resulting in ΔPsbM:ΔPsbY cells being susceptible to photodamage and this required protein synthesis for recovery. Addition of bicarbonate was able to compensate for the light-induced damage in ΔPsbM:ΔPsbY cells potentially re-occupying the modified bicarbonate-binding site in the ΔPsbM:ΔPsbY strain and complementation of ΔPsbM:ΔPsbY cells with the *psbY* gene restored the ΔPsbM phenotype.

Additional key words: assembly; bicarbonate; chlorophyll fluorescence; cytochrome b_{559}; photoinhibition; repair.

Introduction

Photosystem II (PSII) catalyzes the light-driven oxidation of water in oxygenic photosynthesis (Vinyard and Brudvig 2017). A 1.9 Å resolution X-ray-derived crystal structure of PSII is available from the thermophilic cyanobacterium *Thermosynechococcus vulcanus* (Umena *et al.* 2011, Suga *et al*. 2017). The PSII holoenzyme from *T. vulcanus* is dimeric, where each monomer consists of 20 proteins and more than 80 co-factors (Shen 2015). The core of each PSII monomer has four principal polypeptides: these are the two reaction center proteins, D1 and D2, that together bind the majority of the redox cofactors, and two chlorophyll-binding antenna proteins, CP43 and CP47. In the *T. vulcanus* structure, the PSII core is surrounded by 13 low-molecular-weight (LMW) membrane-spanning subunits along with three lumenal proteins (PsbO, PsbU, and PsbV) that cap the site of the Mn_4CaO_5 complex of the catalytic center for oxygen evolution (Bricker *et al.* 2012, Shi *et al.* 2012, Suga *et al.* 2015). Among the LMW proteins, the PsbL, PsbM, and PsbT subunits are located at the monomer–monomer interface of the PSII dimer. PsbY, in contrast, is present at the periphery in proximity to PsbH and between PsbX and the PsbE (or α-chain) of cytochrome b_{559} (Shen 2015, Suga *et al*. 2015) (Fig. 1S, *supplement available online*). Cytochrome b_{559} is formed by two LMW subunits, PsbE and PsbF, and has been ascribed roles in assembly, photoprotection and cyclic electron transfer around PSII (Chu and Chiu 2016).

In this report the role of PsbY has been investigated in the cyanobacterium *Synechocystis* sp. PCC 6803 (hereafter *Synechocystis* 6803). For this study a ΔPsbY knockout mutant (where Δ indicates the absence of the polypeptide) and a double ΔPsbM:ΔPsbY strain have been prepared. Assembly of PSII involves the formation of pre-assembly complexes containing one or more of the D1, D2, CP43, and CP47 proteins which assemble in a stepwise manner to give the mature holoenzyme (Komenda *et al*. 2012).

———

Received 3 October 2017, *accepted* 19 December 2017, *published as online-first* 25 January 2018.
+Corresponding author; email: julian.eaton-rye@otago.ac.nz
Abbreviations: Chl – chlorophyll; CP43 – 43 kDa chlorophyll-binding core antenna protein; CP47 – 47 kDa chlorophyll-binding core antenna protein; DCBQ – 2,6-dichloro-1,4-benzoquinone; DCMU – 3,4-dichloro-1,1-dimethyl urea; DMBQ – 2,5-dimethyl-1,4-benzoquinone; F – fluorescence level; F_m – maximum fluorescence level; F_o – initial fluorescence level; HEPES – 4-(2-hydroxyethyl)-1-piperazineethanesulfonic acid; LMW – low molecular weight; PCC – Pasteur Culture Collection; Q_A – primary plastoquinone electron acceptor of PSII; Q_B – secondary plastoquinone electron acceptor of PS II; RC47 – a PSII pre-assembly complex composed of the reaction center assembly module and the CP47 pre-complex assembly module; S2 – the oxidation state of the oxygen-evolving complex following a single-turnover flash applied to dark-adapted cells; TES – 2-[tris(hydroxymethyl)methyl]amino-1-ethanesulfonic acid.
Acknowledgments: S.B. was supported by an Otago University PhD scholarship. We thank Matthew Prouse for construction of the ΔPsbM and ΔPsbY strains.

PsbM, along with PsbL and PsbT, as well as PsbY, along with PsbH and PsbX, are found as part of the CP47 pre-assembly complex (Boehm *et al.* 2012). The two PsbM subunits of the mature PSII dimer appear to possess a leucine zipper motif suggesting a role in dimer stability; however, dimers still form in the absence of PsbM although the dimer appears to be less stable (Bentley *et al.* 2008, Kawakami *et al.* 2011, Uto *et al.* 2017). Removal of PsbM in *Synechocystis* 6803 also appeared to affect binding of Q_B leading to slightly altered kinetics ascribed to Q_A to Q_B electron transfer (Bentley *et al.* 2008, Uto *et al.* 2017).

Removal of PsbY has been reported to have little impact on PSII activity in *Synechocystis* 6803 but cells lacking PsbY are more sensitive to photoinhibition when stressed under the combination of growth in $CaCl_2$-free media and high light (Meetam *et al.* 1999, Neufeld *et al.* 2004). In this report we set out to investigate the role of PsbY *in vivo* under more moderate conditions by employing a double mutant lacking a second LMW subunit from the CP47 pre-complex. We reasoned that PsbY might be readily lost in the absence of PsbH or PsbX (Kawakami *et al.* 2007, Shen 2015) and that amongst the cluster of LMW subunits at the monomer–monomer interface, removal of PsbM was less disruptive than removal of PsbL or PsbT (Bentley *et al.* 2008). Hence, we selected the construction of the ΔPsbM:ΔPsbY double mutant to probe the role of PsbY in PSII assembly and function.

Materials and methods

Construction of mutants: Overlap extension PCR (Bryksin and Matsumura 2010) was used to delete *psbM* (*sml0003)* and *psbY* (*sml0007)*. For *psbY*, the region between 8 and 117 bp from the start codon was replaced with a kanamycin-resistance cassette and for *psbM*, the region between 4 and 99 bp was replaced with a spectinomycin-resistance cassette (for primers *see* Table S1, *supplement available online*). The PCR generated fragments were then cloned into the *pGEM-T Easy* vector (*Promega*, Madison, WI, USA) and confirmed by sequencing. The plasmids were then used to transform *Synechocystis* 6803 [strain GT-O1 (Morris *et al*. 2014)] to obtain the ΔPsbM, ΔPsbY, and ΔPsbM:ΔPsbY strains. Colony PCR was performed to check the complete segregation of mutants (Fig. 2S, *supplement available online*). The *psbY* gene was also reintroduced into the ΔPsbM:ΔPsbY double mutant to create the complement strain Ycomp. Selection for the incorporation of *psbY* into the Ycomp strain was achieved by inserting a gentamycin-resistance cassette into a unique XbaI site 251 bp downstream of the *psbY* start codon (Fig. 2S).

General growth conditions for strains: Cyanobacteria were maintained on BG-11 plates (1.5% agar), containing atrazine (20 μM), glucose (5 mM), sodium thiosulfate (0.3%), TES-NaOH, pH 8.2 (10 mM), and appropriate antibiotics (kanamycin, 25 μg mL^{-1}; gentamycin, 10 μg mL^{-1}; and spectinomycin, 25 μg mL^{-1}). Plates were kept at 30°C and illuminated with metal halide lamps [30 μmol(photon) m^{-2} s^{-1}]. Liquid starter cultures were grown mixotrophically in modified Erlenmeyer flasks supplemented with 5 mM glucose and antibiotics (Eaton-Rye 2011). Cells were harvested at an optical density at 730 nm ($OD_{730\ nm}$) of 0.8–1.0 (*Thermo Scientific*, *Evolution 201* UV-visible spectrophotometer, Waltham, MA, USA) and collected at 2,760 × *g* for 8 min followed by resuspension in 25 mM HEPES-NaOH (pH 7.5). Chlorophyll (Chl) *a* concentrations were determined according to MacKinney (1941). Cell suspensions were kept at a concentration of 10 μg(Chl) mL^{-1} (unless otherwise noted) in the growth room on a shaker for 30 min after which aliquots were removed and used for each of the physiological experiments described below.

Photoautotrophic growth curves: The harvested cells were washed twice with BG-11 to remove glucose and then flasks, containing 150 mL of BG-11 and appropriate antibiotics, were inoculated with cells at an $OD_{730\ nm}$ of 0.05. During the growth curve the level of media in flasks was maintained by periodic addition of sterile water (resistivity of 18.2 MΩ at 25°C) to account for evaporation.

Variable Chl *a* fluorescence at room temperature: An *FL-3500* kinetic fluorometer (*PSI Instruments*, Brno, Czech Republic) was used to measure the variable Chl *a* fluorescence at room temperature. The cells were prepared as described above and dark-adapted for 8 min prior to measurement. Two milliliters of cells were used for the assay at a final concentration of 5 μg(Chl) mL^{-1}. The measurements were made using blue measuring flashes (455 nm) with a 3-μs duration. The PSII-specific herbicide 3-(3,4-dichlorophenyl)-1,1-dimethylurea (DCMU) was added at 40 μM. The complete protocol for collection and analysis of fluorescence induction data has been described in Jackson *et al.* (2014). For fluorescence relaxation experiments, cells after being dark-adapted were exposed to multiple (up to five) blue actinic flashes (455 nm) at a frequency of 5 Hz. When present, 2,5-dimethy-1,4-benzoquinone (DMBQ), sodium bicarbonate ($NaHCO_3$), sodium formate (HCOONa), and DCMU were added at 250 μM, 15 mM, 25 mM, and 40 μM, respectively.

Oxygen evolution assays: Oxygen-evolution measurements were performed using a Clarke electrode (*Hansatech*, King's Lynn, UK) in the presence of DMBQ (250 μM) or 2,6-dichloro-1,4-benzoquinone (DCBQ, at a final concentration of 200 μM). When DMBQ or DCBQ were used as the primary electron acceptor, 1 mM potassium ferricyanide [$K_3Fe(CN)_6$] was used as a

secondary electron acceptor. If present, DCMU was added at 40 μM. Cells were maintained at a concentration of 10 μg(Chl) mL^{-1}. Other conditions were as described in Jackson *et al.* (2014). When present, bicarbonate was added at 15 mM.

Photodamage assays: Cells, maintained at 10 μg(Chl) mL^{-1}, were exposed to high light [2,000 μmol(photon) m^{-2} s^{-1}] for 45 min and subsequently allowed to recover under low light [30 μmol(photon) m^{-2} s^{-1}]. The total duration of the assay was 3 h with oxygen evolution measured every 15 min in the presence of DMBQ and $K_3Fe(CN)_6$ or in the presence of $NaHCO_3$ at the concentrations stated above. When present lincomycin was added to a final concentration of 500 μg mL^{-1} after the high light period of 45 min.

Low temperature (77 K) fluorescence emission spectroscopy: A modified *MPF-3L* fluorescence spectrophotometer (*Perkin Elmer*, Waltham, MA, USA) adapted to hold a liquid nitrogen Dewar was used to measure the fluorescence emission spectra. Samples were maintained at a concentration of 5 μg(Chl) mL^{-1} in the growth room for at least 30 min and prior to measurement the cells were diluted to a concentration of 2.5 μg(Chl) mL^{-1} and snap frozen in liquid nitrogen. All other details were as described in Jackson *et al.* (2014).

Thylakoid preparation, blue native-polyacrylamide gel electrophoresis and western blotting: Cells were grown mixotrophically with appropriate antibiotics in 1-L Erlenmeyer flasks with constant aeration to an $OD_{730\ nm}$ of 0.8–1.2. The cells were harvested and processed for thylakoid extraction, blue native-polyacrylamide gel electrophoresis (BN-PAGE), and western blotting as described in Jackson *et al.* (2014).

Results

Mutant verification and photoautotrophic growth: The genotypes of each of the mutants were initially confirmed before the photoautotrophic growth of the mutants was compared to wild type (Fig. 2S). The photoautotrophic doubling time for wild type was 12 h while that of the ΔPsbM mutant was 15 h and the doubling time for ΔPsbY was similar at 14 h; however, the ΔPsbM:ΔPsbY double mutant exhibited a doubling time of 17 h (Fig. 1*A*).

PSII activity and assembly: Variable Chl *a* fluorescence induction was measured to initially characterize PSII activity and assembly in the different strains (Stirbet and Govindjee 2011, Stirbet *et al.* 2014). All mutants exhibited similar Chl *a* fluorescence induction kinetics exhibiting a typical O (origin), J (first inflection), I (second inflection), and P (peak) fluorescence trace; however, the extent of the variable fluorescence was reduced resulting in the P level being lower in the mutants relative to wild type (Fig. 1*B*). Furthermore, in the presence of DCMU, the maximum level of variable fluorescence (F_{max}), a potential indicator of the relative level of assembled active PSII centers, was also slightly reduced in the ΔPsbM and ΔPsbM:ΔPsbY strains but was more similar to wild type in ΔPsbY cells (Fig. 1*C*). In addition, following excitation at 440 nm, low (77 K) temperature fluorescence emission at 685 and 695 nm, emanating from PSII (Boehm *et al*. 2011, Jackson *et al.* 2014), was at a similar level relative to the PSI emission at 725 nm in wild type and all mutants (Fig. 2*A*,*B*). Following excitation at 580 nm, however, the emission spectra in the absence of PsbM were quenched relative to spectra obtained with wild type and ΔPsbY cells (Fig. 2*C*,*D*): a reduction was observed for the 685 nm peak and 695 nm shoulder in both ΔPsbM and ΔPsbM:ΔPsbY cells while the ΔPsbM:ΔPsbY mutant also exhibited lower 650 nm and 665 nm emission peaks relative to the other strains.

To independently assess the relative level of assembled centers in the different strains BN-PAGE was performed on isolated thylakoids. The relative amounts of PSII dimers and monomers were detected using specific antibodies to the D1, D2, CP43, and CP47 proteins. In strains lacking PsbY, a slight reduction in the amount of PSII dimers relative to wild type and the ΔPsbM strain was apparent (Fig. 3). In addition, the RC47 pre-complex was observed to accumulate to a greater extent in strains lacking PsbM: an observation also reported by Bentley *et al.* (2008). In this experiment, putative pre-assembly complexes containing either CP43 or CP47 were also detected in all strains. This included an additional CP43-containing complex that was unique to both strains that lacked PsbM (Fig. 3*D*).

PSII activity in the different strains was also determined using the artificial quinone electron acceptors DMBQ and DCBQ. In the presence of DMBQ both single and double mutants showed a slight reduction in oxygen evolution rates compared to the wild type (Fig. 4*A*). The observed rates of oxygen evolution were 380, 285, 299, and 301 μmol(O_2) mg(Chl) $^{-1}$ h^{-1} for wild type and the ΔPsbM, ΔPsbY, and ΔPsbM:ΔPsbY mutants, respectively. In the presence of DCBQ (Fig. 4*B*), enhanced rates of oxygen evolution, relative to the rates observed with DMBQ, were observed. In the presence of DCBQ, the observed rates of oxygen evolution were 529, 489, 348, and 375 μmol(O_2) mg(Chl) $^{-1}$ h^{-1} for wild type and the ΔPsbM, ΔPsbY, and ΔPsbM:ΔPsbY mutants, respectively. The enhanced rates observed in the presence of DCBQ prompted us to also determine the effect of DCMU addition on oxygen evolution (Fig. 4*C*,*D*). Interestingly, strains lacking PsbM exhibited DCMU-insensitive oxygen evolution when DCBQ was present as the electron acceptor and this effect was most pronounced in ΔPsbM:ΔPsbY cells. In contrast, DCMU blocked oxygen evolution in all strains in the presence of DMBQ. We therefore selected DMBQ as the PSII-specific electron acceptor in our photodamage assays.

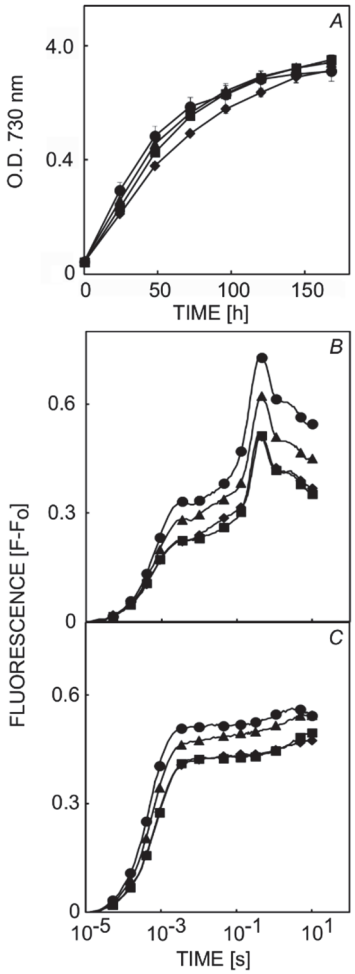

Fig. 1. (*A*) Photoautotrophic growth as measured by the optical density at 730 nm. The cell volume was 150 mL and the light intensity was [30 µmol(photon) m^{-2} s^{-1}]. (*B*) Variable chlorophyll (Chl) *a* fluorescence induction. (*C*) Variable Chl *a* fluorescence induction in the presence of DCMU. Wild type (*circles*), ΔPsbM (*squares*), ΔPsbY (*triangles*), and ΔPsbM:ΔPsbY (*diamonds*). F is the fluorescence level at the specified times and F_o is the initial fluorescence level. For clarity only selected data points are shown in panels *B* and *C*. All results are the average of three individual biological replicates. Error bars in panel *A* are the standard error and error bars smaller than the symbols are not shown.

Photodamage assays: We tested if removal of PsbY could influence the susceptibility of *Synechocystis* 6803 cells to photodamage or recovery from high-light-induced damage. Cells were subjected to high light [2,000 µmol(photon) m^{-2} s^{-1}] for 45 min and then allowed to recover under low light [30 µmol(photon) m^{-2} s^{-1}]. When using DMBQ/ $K_3Fe(CN)_6$ as the PSII-specific electron-accepting system, wild type and the ΔPsbM and ΔPsbY cells were able to acclimate to the high-light exposure and rates of oxygen evolution remained close to the rates obtained before the high light was applied. In contrast, the rate of oxygen evolution in the ΔPsbM:ΔPsbY strain dropped by ~50% in the first 15 min of exposure to high light and then remained

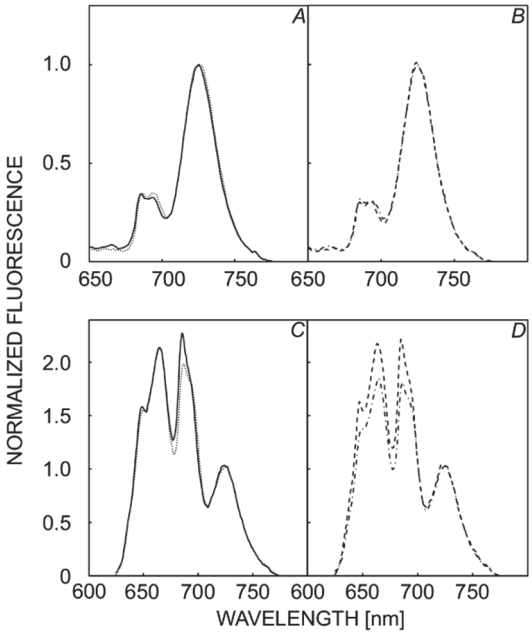

Fig. 2. Low temperature (77 K) fluorescence emission spectra following excitation at 440 nm for (*A*) wild type and ΔPsbM, and (*B*) ΔPsbY and ΔPsbM:ΔPsbY. Low temperature (77 K) fluorescence emission spectra following excitation at 580 nm of (*C*) wild type and ΔPsbM, and (*D*) ΔPsbY and ΔPsbM:ΔPsbY. Wild type (continuous line); ΔPsbM (dots); ΔPsbY (dashes); ΔPsbM:ΔPsbY (dashes and dots). Results are the average of three individual biological replicates. All spectra were normalized to the fluorescence emission from PSI at 725 nm.

at ~40% of the initial rate until the cells were returned to low light conditions, upon which they recovered with a half-time of ~35 min (Fig. 5*A*). Notably, for all strains, the rate of oxygen evolution attained upon returning to low light conditions exceeded the rates observed at the onset of the experiment before the high light had been applied. In Fig. 5*B* the experiment was repeated but lincomycin was added after the high-light treatment. In the presence of the protein synthesis inhibitor, the recovery of PSII activity under low light was prevented. Additionally, in the experiment in Fig. 5*B* a fresh bulb was used in the slide projector that supplied the high light. In the presence of the new light bulb, the extent of high-light-induced inhibition increased and we ascribe this to a change in light quality between the old and new bulbs.

We also tested if the sensitivity of the ΔPsbM:ΔPsbY cells was solely the result of the absence of PsbY by reintroducing a functional *psbY* gene into the double mutant to create a complimented ΔPsbM:ΔPsbY strain denoted as the Ycomp mutant. In Fig. 5*A,* the Ycomp strain was observed to be similar to the single mutant and the wild type indicating that the high light sensitivity was due to the absence of PsbY. In addition, we also repeated the experiment using bicarbonate to support whole chain electron transport. In Fig 5*C* it can be seen that PSII activity, when supported by the native quinone, was not

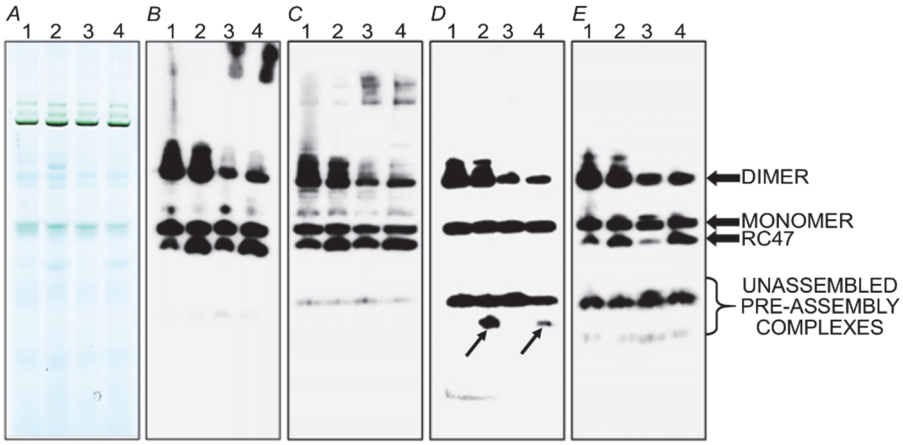

Fig. 3. Analysis of PSII assembly by BN-PAGE and western blotting. Wild type (lane 1), ΔPsbM (lane 2), ΔPsbY (lane 3), and ΔPsbM:ΔPsbY (lane 4). The different assembly complexes were separated in (*A*) on a 3–12% gradient gel, followed by identification using antibodies raised against the core reaction center proteins: D1 (*B*), D2 (*C*), CP43 (*D*), and CP47 (*E*). The arrows in panel D indicate an additional putative CP43-containing unincorporated complex in strains lacking PsbM.

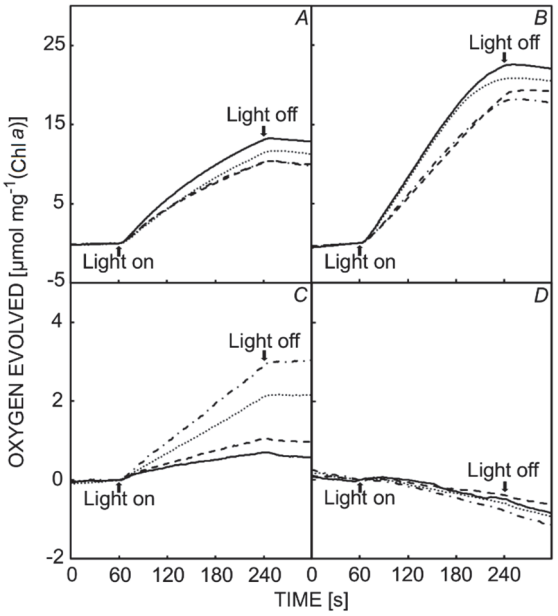

Fig. 4. Oxygen evolution traces in the presence of (*A*) DMBQ and $K_3Fe(CN)_6$, (*B*) DCBQ and $K_3Fe(CN)_6$, (*C*) DCBQ, DCMU, and $K_3Fe(CN)_6$, and (*D*) DMBQ, DCMU, and $K_3Fe(CN)_6$. Wild type (*continuous line*); ΔPsbM (*dots*); ΔPsbY (*dashes*); ΔPsbM: ΔPsbY (*dashes and dots*). Traces in panels *A*, *B*, and *C* are the average of three independent experiments; traces in panel *D* are the average of two independent experiments. The observed rates of oxygen evolution (*see* text) were reproducible to within 15% of the avearge.

impaired when high light was applied. Oxygen evolution was also not impaired when bicarbonate was added to the assay in the presence of the DMBQ/$K_3Fe(CN)_6$ electron-accepting system (Fig. 3S, *supplement available online*). The differences observed between oxygen evolution supported by either DMBQ or bicarbonate, together with the differential effect of DCMU on PSII oxygen evolution supported by DMBQ or DCBQ (Fig. 4*C,D*), suggested that the acceptor side of PSII was altered in our mutants. To investigate this, we measured the decay of variable fluorescence following single turnover actinic flashes as a probe of electron transfer between Q_A and Q_B (Robinson and Crofts 1983, Vass *et al.* 1999).

PSII acceptor side activity probed by the decay of variable Chl *a* fluorescence following single or multiple actinic flashes: Following a saturating actinic flash the decay kinetics of the variable Chl *a* fluorescence can be divided into three components: a fast microsecond phase ascribed to forward electron transfer from Q_A^- to Q_B, an intermediate millisecond component resulting from the binding of plastoquinone to the Q_B-binding site, and one slow seconds phase ascribed to a back reaction consisting of charge recombination between Q_A^- and the donor side of PSII (Robinson and Crofts 1983, Vass *et al.* 1999). The decay of Chl *a* fluorescence for each of the strains following a single actinic flash is shown in Fig. 6*A* and the analysis of the kinetics is shown in Table 1. In each of the mutants, the fast phase is somewhat slowed relative to wild type and this is accompanied, particularly in the ΔPsbM strain and in the ΔPsbM:ΔPsbY mutant, by an increase in the half time for the milliseconds component [from 2.6 ms (31%) in wild type to 5.2 ms (24%) in ΔPsbM cells and 10.7 ms (21%) in the ΔPsbM:ΔPsbY double mutant]. Moreover, the increased millisecond component in the double mutant was reversed to resemble the rate and amplitude of the single ΔPsbM strain in the Ycomp cells. In Fig. 6*B,* the decay of the Chl *a* fluorescence following a single actinic flash, in the presence of DCMU, is shown and the kinetic analysis is presented in Table 1. A biphasic decay was observed with the amplitude of an initial millisecond component increased in the mutants but this effect was not reversed in the Ycomp strain.

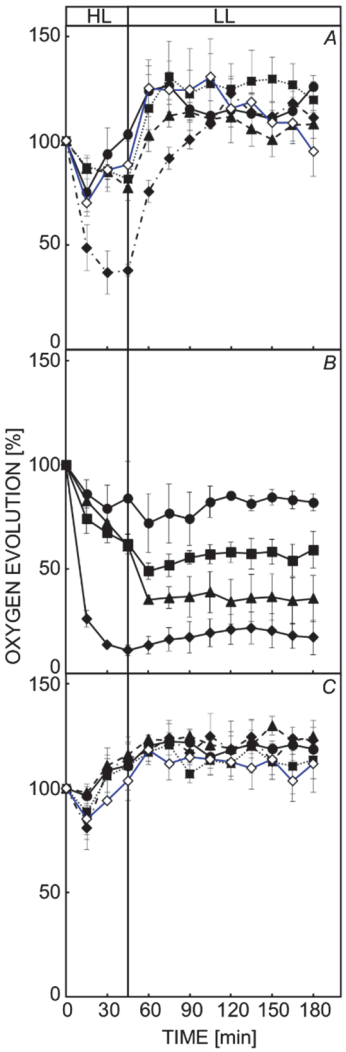

Fig. 5. Photodamage and recovery assay: Cells were subjected to 45 min of high light (HL) [2 mmol(photon) m^{-2} s^{-1}] followed by low light (LL) [30 µmol(photon) m^{-2} s^{-1}]. Oxygen evolution was measured in the presence of (*A*) DMBQ and $K_3Fe(CN)_6$, (*B*) DMBQ and $K_3Fe(CN)_6$ with lincomycin added at 500 µg mL^{-1} after the HL treatment. (*C*) Sodium bicarbonate (15 mM). Wild type (*circles*), ΔPsbM (*squares*), ΔPsbY (*triangles*), ΔPsbM: ΔPsbY (*diamonds*), and ΔPsbM:ΔPsbY complemented with PsbY (Ycomp) (*open diamonds, blue line*). Data are the average of three biological replicates. Error bars are the standard error and error bars smaller than the symbols are not shown.

The influence of DMBQ on the Chl *a* fluorescence decay was also investigated after 1 actinic flash in Fig. 6*C* and the kinetics analyzed in Table 2. Notably the half-time of the millisecond component was increased by two-fold in the absence of PsbM but the half time was not affected by the removal of PsbY; however, the removal of PsbY accelerated the decay of the slow seconds component, indicative of an enhanced back reaction pathway in cells lacking PsbY when DMBQ is present. Interestingly, the observed accelerated slow component was slowed by the addition of bicarbonate to the reaction (Table 2). A bicarbonate ion is bound to the non-heme iron located between Q_A and Q_B in PSII (Umena *et al*. 2011, Shevela *et al*. 2012): and removal of bound bicarbonate, or replacing it by addition of formate, slows Q_A^- oxidation (Eaton-Rye and Govindjee 1988a,b, Sedoud *et al.* 2011). We therefore investigated the effect of bicarbonate-reversible formate-induced inhibition of Q_A^- oxidation in ΔPsbM, ΔPsbY, and ΔPsbM:ΔPsbY cells (Figs. 6*E*,*F*; Table 3). Addition of formate had the effect of slowing the kinetics of the fast and intermediate components in the wild type and single mutants to resemble the rates observed for the double mutant without addition of either DMBQ or formate and this effect was reversible in all strains except the ΔPsbM:ΔPsbY double mutant (Table 3). The slow component was also accelerated in all strains by the presence of formate to be on the order of 1 s but restored to ~10 s in wild type and the ΔPsbM and Ycomp strains upon addition of bicarbonate; however, the half time of the slow component remained at approximately 6 or 8 s in both strains lacking PsbY. In addition, we observed that the inhibitory effects observed following either the addition of DMBQ or formate were exacerbated following multiple turnovers of the acceptor side when up to five actinic flashes were supplied at 5 Hz (Figs. 4S and 5S, *supplements available online*).

Discussion

The PsbY protein is adjacent to the α (PsbE) and β (PsbF) subunits of cytochrome b_{559} in cyanobacteria (Kawakami *et al.* 2007, Shen 2015), red algae (Ago *et al.* 2016), and plants (Wei *et al.* 2016). This position, at the periphery of the complex, is therefore unconnected with PsbM located at the monomer–monomer interface (Umena *et al.* 2011). Removal of PsbY did not appear to alter PSII assembly to any great extent in the ΔPsbY strain beyond the noted reduction in the level of dimers (Figs. 2, 3); however, the incorporation of CP43 into the RC47 complex lacking PsbM was impaired and in both ΔPsbM and ΔPsbM:ΔPsbY cells an additional pre-complex containing CP43 was observed in the thylakoid membranes isolated in this study (Fig. 3).

Table 1. Decay kinetics of flash-induced variable fluorescence in the presence and absence of DCMU. $T_{1/2}$ – half time; A – amplitude.

		$T_{1/2}$ [μs]	A [%]	$T_{1/2}$ [ms]	A [%]	$T_{1/2}$ [s]	A [%]
No addition	Wild type	267 ± 19	61 ± 2	2.6 ± 0.3	30.9 ± 1.2	5.5 ± 0.4	7.7 ± 0.5
	ΔPsbM	332 ± 3	64 ± 1	5.2 ± 0.2	23.5 ± 0.5	7.0 ± 1.0	12.5 ± 0.9
	ΔPsbY	331 ± 13	62 ± 1	3.9 ± 0.4	29.6 ± 1.1	6.2 ± 0.3	8.6 ± 0.3
	ΔPsbM:ΔPsbY	408 ± 12	66 ± 1	10.7 ± 2	20.6 ± 1.3	6.6 ± 0.9	13.6 ± 0.7
	Ycomp	403 ± 11	63 ± 1	6.2 ± 0.3	26.5 ± 0.5	11.1 ± 0.3	10.5 ± 0.3
DCMU	Wild type			1.6 ± 0.4	6.9 ± 1.0	0.5 ± 0.02	93.2 ± 1.0
	ΔPsbM			1.4 ± 0.1	9.4 ± 1.2	0.6 ± 0.04	90.6 ± 1.2
	ΔPsbY			1.7 ± 0.4	8.8 ± 1.7	0.4 ± 0.02	91.3 ± 1.7
	ΔPsbM:ΔPsbY			1.7 ± 0.4	14.4 ± 0.9	0.6 ± 0.02	85.6 ± 0.9
	Ycomp			2.4 ± 0.1	12.1 ± 0.2	0.6 ± 0.01	87.9 ± 0.2

Table 2. Decay kinetics of flash-induced variable fluorescence in the presence of DMBQ and DMBQ with bicarbonate. $T_{1/2}$ – half time; A – amplitude..

		$T_{1/2}$ [μs]	A [%]	$T_{1/2}$ [ms]	A [%]	$T_{1/2}$ [s]	A [%]
DMBQ	Wild type	282 ± 37	60 ± 2	7.5 ± 1.9	25.5 ± 1.4	6.3 ± 0.1	14.5 ± 0.2
	ΔPsbM	365 ± 9	54 ± 4	15 ± 1.7	23.5 ± 0.5	5.4 ± 1.3	22.1 ± 3.7
	ΔPsbY	352 ± 18	52 ± 1	7.6 ± 0.7	26.3 ± 1.0	2.7 ± 0.1	21.5 ± 0.9
	ΔPsbM:ΔPsbY	415 ± 13	47 ± 5	15.3 ± 0.9	21.8 ± 0.4	1.8 ± 0.2	31.6 ± 5.1
	Ycomp	396 ± 3	48 ± 0.5	12.6 ± 0.9	26.5 ± 0.3	6.0 ± 0.3	25.8 ± 0.3
DMBQ + bicarbonate	Wild type	233 ± 41	60 ± 2	6.1 ± 2.3	26.6 ± 1.9	11.0 ± 0.8	13.0 ± 0.2
	ΔPsbM	288 ± 36	55 ± 1	11.8 ± 2.4	26.1 ± 0.3	13.3 ± 2.9	19.3 ± 0.6
	ΔPsbY	250 ± 24	55 ± 0.3	6.1 ± 1.8	29.0 ± 0.8	7.3 ± 0.4	15.8 ± 0.4
	ΔPsbM:ΔPsbY	313 ± 14	52 ± 1	14.2 ± 2.3	24.6 ± 0.4	7.0 ± 1.0	23.7 ± 0.8
	Ycomp	309 ± 13	52 ± 0.4	9.9 ± 0.5	27.1 ± 0.4	11.8 ± 0.2	21.0 ± 0.2

Table 3. Decay kinetics of flash-induced variable fluorescence in the presence of 25 mM formate and 25 mM formate with 15 mM bicarbonate. $T_{1/2}$ – half time; A – amplitude..

		$T_{1/2}$ [μs]	A [%]	$T_{1/2}$ [ms]	A [%]	$T_{1/2}$ [s]	A [%]
Formate	Wild type	423 ± 33	57 ± 3	8.6 ± 0.8	28.6 ± 1.8	1.4 ± 0.2	14.4 ± 1.6
	ΔPsbM	443 ± 12	50 ± 2	9.3 ± 0.4	28.7 ± 0.9	1.3 ± 0.03	20.9 ± 0.8
	ΔPsbY	455 ± 7	51 ± 5	9.7 ± 0.4	32.5 ± 2.4	1.2 ± 0.3	16.8 ± 2.6
	ΔPsbM:ΔPsbY	469 ± 17	52 ± 2	12.3 ± 2.2	28.3 ± 0.3	1.5 ± 0.6	19.9 ± 1.7
	Ycomp	537 ± 13	45 ± 1	12.0 ± 0.3	32.7 ± 0.2	1.4 ± 0.1	21.8 ± 0.7
Formate + bicarbonate	Wild type	282 ± 23	65 ± 1	3.9 ± 0.3	26.8 ± 0.8	11.3 ± 1.0	8.5 ± 0.1
	ΔPsbM	302 ± 5	65 ± 1	5.5 ± 0.9	24.3 ± 0.9	9.6 ± 0.4	11.1 ± 0.01
	ΔPsbY	303 ± 17	62 ± 0.4	4.3 ± 0.4	28.6 ± 0.8	5.7 ± 1.0	9.0 ± 0.4
	ΔPsbM:ΔPsbY	358 ± 16	64 ± 1	12.3 ± 3.2	22.7 ± 0.6	7.7 ± 0.6	13.5 ± 0.8
	Ycomp	380 ± 13	64 ± 1	7.6 ± 0.8	25.4 ± 1.0	12.0 ± 0.5	10.9 ± 0.2

We previously constructed a ΔPsbM strain in *Synechocystis* 6803 that exhibited susceptibility to high light (Bentley *et al.* 2008); however, subsequent analysis revealed that a second mutation was present in this strain in the ChlH subunit of magnesium chelatase that has been shown to additionally impair PSII activity in specific mutants by restricting the supply of chlorophyll (Morris *et al.* 2014, Crawford *et al.* 2016). We therefore utilized a new ΔPsbM strain in this study which was able to maintain its oxygen evolution rates when exposed to high light (Fig. 5*A*) but with a similar phenotype to a ΔPsbM strain from *T. vulcanus* obtained by Uto *et al.* (2017), exhibiting impaired electron flow between Q_A and Q_B and potentially possessing an altered Q_B-binding site (Table 1, Fig. 6, Figs. 4S, 5S).

Evidence for an altered acceptor side in our ΔPsbM strain was also obtained from PSII activity measurements in the presence of DCMU (a PSII-specific inhibitor) in which oxygen evolution was supported by DCBQ/ $K_3Fe(CN)_6$ but not by DMBQ/$K_3Fe(CN)_6$ (Fig. 4). In

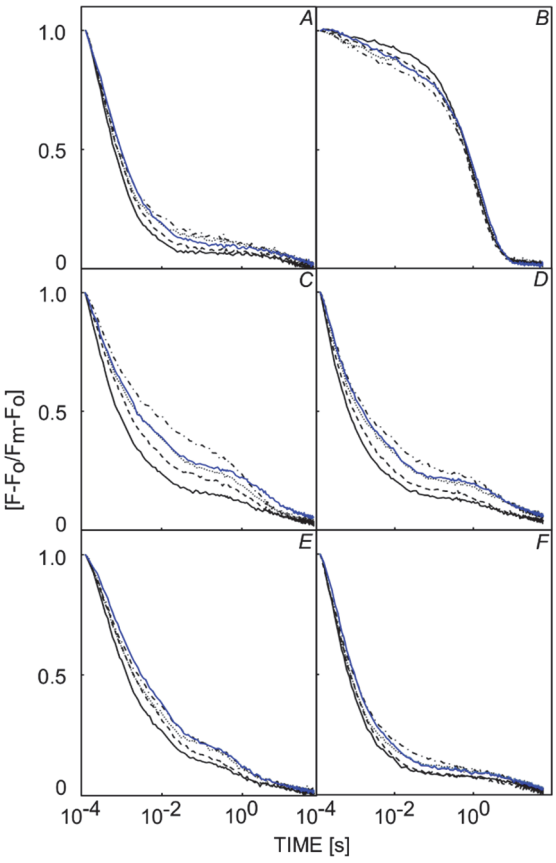

Fig. 6. Relaxation of chlorophyll *a* fluorescence after a saturating actinic flash. (*A*) No addition, (*B*) in the presence of DCMU, (*C*) in the presence of DMBQ, (*D*) in the presence of DMBQ and sodium bicarbonate, (*E*) in the presence of sodium formate, and (*F*) in the presence of sodium formate and sodium bicarbonate. Wild type (black line); ΔPsbM (dots); ΔPsbY (dashes); ΔPsbM: ΔPsbY (dashes and dots), and Ycomp (blue line). Data are the average of three biological replicates. F is the fluorescence level at the specified times and F_m and F_o are the maximum and intial fluorescence levels, respectively.

addition, the millisecond component for the decay of Chl fluorescence after a single turnover actinic flash in the ΔPsbM:ΔPsbY mutant increased from 5.2 ms in ΔPsbM cells to 11 ms and the double mutant exhibited the highest rates of DCMU-insensitive electron transfer to DCBQ: hence, removing PsbY introduced further changes at the acceptor side of PSII in ΔPsbM cells despite being ~50 Å from the Q_B-binding site (Table 1, Figs. 4, 6; Figs. 4S, 5S).

Oxygen evolution by ΔPsbM:ΔPsbY cells supported by DMBQ/$K_3Fe(CN)_6$ was inactivated by high light and recovery of these cells under low light required protein synthesis (Fig. 5). This phenomenon was not observed when oxygen evolution was supported by the addition of bicarbonate. This may reflect the fact that the native quinone is accepting electrons under these conditions as suggested for a similar observation in cells carrying a mutation in the cytosolic de loop of the D1 protein (Nixon *et al.* 1995). However, if bicarbonate binding to the non-heme iron of PSII in ΔPsbM cells is disrupted it could potentially favor bicarbonate release during the high-light treatment and this would be expected to inhibit electron transfer (Shevela *et al.* 2012, Brinkert *et al.* 2016, Uto *et al.* 2017). It is therefore possible that the millimolar concentrations of bicarbonate added in our oxygen evolution assays were sufficient to re-occupy the bicarbonate site and compensate for the light-induced inactivation observed when DMBQ is used as the electron acceptor.

Formate has been shown to displace bicarbonate in PSII slowing Q_A to Q_B electron transfer (Robinson *et al.* 1984, Eaton-Rye *et al.* 1988a,b, Sedoud *et al.* 2011). Notably bicarbonate could not restore the millisecond component in ΔPsbM:ΔPsbY cells in the presence of formate to resemble the rate observed in wild type (Table 3); however, the addition of bicarbonate did reverse the kinetics of the seconds component to resemble the rate and amplitude of this component in untreated ΔPsbM:ΔPsbY cells (*cf.* Table 1). This would appear to suggest that the removal of PsbY in ΔPsbM cells has a greater deleterious effect on forward electron transfer from Q_A^- than with the back reaction with the S2 state of the oxygen-evolving complex. Another possibility is that the addition of bicarbonate facilitates a different slow pathway of Q_A^- oxidation. The slow seconds component may represent a pathway involving an alternative electron acceptor consistent with the report that removal of PsbY can modify the redox potential of cytochrome b_{559} (von Sydow *et al.* 2016). This latter interpretation would be consistent with the susceptibility of ΔPsbM:ΔPsbY cells to photodamage arising from impairment of the alternative pathway and the reversibility of this phenomenon either upon addition of bicarbonate or by complementation of the ΔPsbM:ΔPsbY strain with PsbY.

Conclusions: Removal of PsbM resulted in the persistance of a CP43-containing pre-complex not seen in isolated thylakoids from wild type or ΔPsbY cells and also increased the observable level of the RC47 complex in these membranes. In addition, the absence of PsbM disrupted the Q_B-binding site and potentially also bicarbonate binding to the non-heme iron, consistent with the observations of Uto *et al.* (2017). Removal of PsbY in the ΔPsbM strain led to additional modification of the acceptor side that resulted in ΔPsbM:ΔPsbY cells being susceptible to photodamage and this required protein synthesis for recovery. However, the addition of bicarbonate was able to compensate for the light-induced damage in the ΔPsbM:ΔPsbY strain by potentially re-occupying a modified bicarbonate-binding site in the ΔPsbM:ΔPsbY cells.

References

Ago H., Adachi H., Umena Y. *et al.*: Novel features of eukaryotic Photosystem II revealed by its crystal structure analysis from a red alga. – J. Biol. Chem. **291**: 5676-5687, 2016.

Bentley F.K., Luo H., Dilbeck P. *et al.*: Effects of inactivating *psbM* and *psbT* on photodamage and assembly of Photosystem II in *Synechocystis* sp. PCC 6803. – Biochemistry **47**: 11637-11646, 2008.

Boehm M., Yu J., Reisinger V. *et al.*: Subunit composition of CP43-less Photosystem II complexes of *Synechocystis* sp. PCC 6803: implications for the assembly and repair of Photosystem II. – Phil. T. Roy. Soc. B **367**: 3444-3454, 2012.

Boehm M., Romero E., Reisinger V. et al.: Investigating the early stages of Photosystem II assembly in *Synechocystis* sp. PCC 6803: isolation of CP47 and CP43 complexes. – J. Biol. Chem. **286**: 14812-14819, 2011.

Bricker T.M., Roose J.L., Fagerlund R.D. *et al.*: The extrinsic proteins of Photosystem II. – Biochim. Biophys. Acta **1817**: 121-142, 2012.

Brinkert K., Causmaecker S.D., Krieger-Liszkay A. *et al.*: Bicarbonate-induced redox tuning in Photosystem II for regulation and protection. – P. Natl. Acad. Sci. USA **113**: 12144-12149, 2016.

Bryksin A.V., Matsumura I.: Overlap extension PCR cloning: A simple and reliable way to create recombinant plasmids. – Biotechniques **48**: 463-465, 2010.

Chu H.-A., Chiu Y.-F.: The roles of cytochrome b_{559} in assembly and photoprotection of Photosystem II revealed by site-directed mutagenesis studies. – Front. Plant Sci. **6**: 1261, 2016.

Crawford T.S., Eaton-Rye J.J., Summerfield T.C.: Mutation of Gly195 of the ChlH subunit of Mg-chelatase reduces chlorophyll and further disrupts PS II assembly in a Ycf48-deficient strain of *Synechocystis* sp. PCC 6803. – Front. Plant Sci. **7**: 1060, 2016

Eaton-Rye J.J.: Construction of gene interruptions and gene deletions in the cyanobacterium *Synechocystis* sp. strain PCC 6803. – Methods Mol. Biol. **684**: 295-312, 2011.

Eaton-Rye J.J., Govindjee: Electron transfer through the quinone acceptor complex of Photosystem II in bicarbonate-depleted spinach thylakoid membranes as a function of actinic flash number and frequency. – BBA-Bioenergetics **935**: 237-247, 1988a.

Eaton-Rye J.J., Govindjee: Electron transfer through the quinone accepter complex of Photosystem II after one or two actinic flashes in bicarbonate-depleted spinach thylakoid membranes. – BBA-Bioenergetics **935**: 248-257, 1988b.

Jackson S.A., Hervey J.R.D., Dale A.J. *et al.*: Removal of both Ycf48 and Psb27 in *Synechocystis* sp. PCC 6803 disrupts Photosystem II assembly and alters Q_A^- oxidation in the mature complex. – FEBS Lett. **588**: 3751-3760, 2014.

Kawakami K., Iwai M., Ikeuchi M. *et al.*: Location of PsbY in oxygen-evolving Photosystem II revealed by mutagenesis and X-ray crystallography. – FEBS Lett. **581**: 4983-4987, 2007.

Kawakami K., Umena Y., Iwai M. *et al.*: Roles of PsbI and PsbM in Photosystem II dimer formation and stability studied by deletion mutagenesis and X-ray crystallography. – Biochim. Biophys. Acta **1807**: 319-325, 2011.

Komenda J., Sobotka R., Nixon P.J.: Assembling and maintaining the Photosystem II complex in chloroplasts and cyanobacteria. – Curr. Opin. Plant Biol. **15**: 245-251, 2012.

MacKinney G.: Absorption of light by chlorophyll solutions. – J. Biol. Chem. **140**: 315-322, 1941.

Meetam M., Keren N., Ohad I. *et al.*: The PsbY protein is not essential for oxygenic photosynthesis in the cyanobacterium *Synechocystis* sp. PCC 6803. – Plant Physiol. **121**: 1267-1272, 1999.

Morris J.N., Crawford T.S., Jeffs A. *et al.*: Whole genome re-sequencing of two "wild-type" strains of the model cyanobacterium *Synechocystis* sp. PCC 6803. – New Zeal. J. Bot. **52**: 36-47, 2014.

Neufeld S., Zinchenko V., Stephan D.P. *et al.*: On the functional significance of the polypeptide PsbY for photosynthetic water oxidation in the cyanobacterium *Synechocystis* sp. strain PCC 6803. – Mol. Genet. Genomics **271**: 458-467, 2004.

Nixon P.J., Komenda J., Barber J. *et al.*: Deletion of the PEST-like region of photosystem two modifies the Q_B-binding pocket but does not prevent rapid turnover of D1. – J. Biol. Chem. **270**: 14919-14927, 1995.

Robinson H.H., Crofts A.R.: Kinetics of the oxidation-reduction reactions of the Photosystem II quinone acceptor complex, and the pathway for deactivation. – FEBS Lett. **153**: 221-226, 1983.

Robinson, H.H., Eaton-Rye, J.J., van Resen, J.J.S., Govindjee.: The effects of bicarbonate depletion and formate incubation on the kinetics of oxidation-reduction reactions of the Photosystem II quinone acceptor complex. – Z. Naturforsch. **39c**: 382-385, 1984.

Sedoud A., Kastner L., Cox N. *et al.*: Effects of formate binding on the quinone-iron electron acceptor complex of Photosystem II. – Biochim. Biophys. Acta **1807**: 216-226, 2011.

Shen J.-R.: The structure of Photosystem II, and the mechanism of water oxidation in photosynthesis. – Annu. Rev. Plant Biol. **66**: 23-48, 2015.

Shi L.-X., Hall M., Funk C. *et al.*: Photosystem II, a growing complex: updates on newly discovered components and low molecular mass proteins. – Biochim. Biophys. Acta **1817**: 13-25, 2012.

Shevela D., Eaton-Rye J.J., Shen J.-R., Govindjee: Photosystem II and the unique role of bicarbonate: A historical perspective. – Biochim. Biophys. Acta **1817**: 1134-1151, 2012.

Stirbet A., Govindjee: On the relation between the Kautsky effect (chlorophyll *a* fluorescence induction) and Photosystem II: Basics and applications of the OJIP fluorescence transient. – J. Photochem. Photobiol. B **104**: 236-257, 2011.

Stirbet A., Riznichenko G.Y., Rubin A.B. *et al.*: Modeling chlorophyll *a* fluorescence transient : relation to photosynthesis. – Biochemistry-Moscow **79**: 291-323, 2014.

Suga M., Akita F., Hirata K. *et al.*: Native structure of Photosystem II at 1.95 Å resolution viewed by femtosecond X-ray pulses. – Nature **517**: 99-103, 2015.

Suga M., Akita F., Sugahara M. *et al.*: Light-induced structural changes and the site of O = O bond formation in PSII caught by XFEL. – Nature **543**:131-135, 2017.

Umena Y., Kawakami K., Shen J.-R. *et al.*: Crystal structure of oxygen-evolving Photosystem II at a resolution of 1.9 Å. – Nature **473**: 55-60, 2011.

Uto S., Kawakami K., Umena Y. *et al.*: Mutational relationships between structural and functional changes in a PsbM-deletion mutants of Photosystem II. – Faraday Discuss. **198**: 107-120, 2017.

Vass I., Kirilovsky D., Etienne A.: UV-B radiation-induced donor- and acceptor-side modifications of Photosystem II in the cyanobacterium *Synechocystis* sp. PCC 6803. – Biochemistry **38**: 12786-12794, 1999.

Vinyard D.J., Brudvig G.W.: Progress towards a molecular mechanism of water oxidation in Photosystem II. – Annu. Rev. Phys. Chem. **68**: 101-116, 2017.

von Sydow L.V., Schwenkert S., Meurer J. *et al*.: The PsbY protein of *Arabidopsis* Photosystem II is important for the redox control of cytochrome b_{559}. – Biochem. Biophys. Acta **1857**: 1524-1533, 2016.

Wei X., Su X., Cao P. *et al*.: Spinach Photosystem II-LHCII supercomplex at 3.2 Å resolution. – Nature **534**: 69-74, 2016.